Review

Oxyfluoride Chemistry of Layered Perovskite Compounds

Yoshihiro Tsujimoto [1],*, Kazunari Yamaura [2,3] and Eiji Takayama-Muromachi [2,3]

[1] International Center for Young Scientists (ICYS), International Center for Materials Nanoarchitechtonics (WPI-MANA), National Institute for Materials Science (NIMS)/Namiki 1-1, Tsukuba, Ibaraki 305-0044, Japan

[2] Superconducting Properties Unit, NIMS/Namiki 1-1, Tsukuba, Ibaraki 305-0044, Japan; E-Mails: yamaura.kazunari@nims.go.jp (K.Y.); muromachi.eiji@nims.go.jp (E.T.-M.)

[3] JST (Japan Science and Technol- ogy Agency), Transformative Research-Project on Iron Pnictides (TRIP)/Namiki 1-1, Tsukuba, Ibaraki 305-0044, Japan

* Author to whom correspondence should be addressed; E-Mail: TSUJIMOTO.Yoshihiro@nims.go.jp; Tel.: +81-29-851-3354; Fax: +81-29-860-4706.

Abstract: In this paper, we review recent progress and new challenges in the area of oxyfluoride perovskite, especially layered systems including Ruddlesden-Popper (RP), Dion-Jacobson (DJ) and Aurivillius (AV) type perovskite families. It is difficult to synthesize oxyfluoride perovskite using a conventional solid-state reaction because of the high chemical stability of the simple fluoride starting materials. Nevertheless, persistent efforts made by solid-state chemists have led to a major breakthrough in stabilizing such a mixed anion system. In particular, it is known that layered perovskite compounds exhibit a rich variety of O/F site occupation according to the synthesis used. We also present the synthetic strategies to further extend RP type perovskite compounds, with particular reference to newly synthesized oxyfluorides, Sr_2CoO_3F and $Sr_3Fe_2O_{5+x}F_{2-x}$ ($x \sim 0.44$).

1. Introduction

Since the discovery of a high-T_C superconducting cuprate by Bednorz and Muller [1], there has been considerable progress in the field of solid-state chemistry and physics. In particular, we have deepened the understanding of metal oxides, while making improvements and development of experimental techniques and theories. It is well known that a perovskite structure formulated as ABO_3 (*A* = large *s*-, *d*-, or *f*-block cation; *B* = smaller transition metal cation) has rich variety in structural, electronic and magnetic properties, ranging from superconductivity, through ferroelectricity, to photocatalytic activity. Figure 1(a) shows the ideal perovskite structure in which *A* cation occupies an interstitial site of an eight corner-sharing BO_6 octahedra. This type of structure can be extended to the layered perovskite intergrowth system termed the Ruddlesden-Popper (RP) phase, $A_2A'_{n-1}B_nO_{3n+1}$ (*n* = the number of perovskite block), the structures with *n* = 1 and 2 which are depicted in Figure 1(b) and (c). Each perovskite block is intervened with double rock-salt *A*O layers. Thanks to the ability of the *A* and *B* sites to adopt various metal cations, we are able to finely control the chemical compositions as well as the physical properties, as exemplified by magnetoresistive manganite [2–4] and superconducting cuprate [5,6]. While the majority of studies have concentrated on the influence of cation substitution, little effort has been made to control the structural and physical properties by manipulating the anion lattices. Considering that the anion strongly affects the crystal field and electronic state of the metal center, we can expect that substitution of anions with different bonding nature, valence state or ionic radius from oxygen in a metal oxide can enhance the original physical properties or induce new exotic phenomena. In fact, $LaTiO_2N$ [7] and $Sr_2CuO_2F_{2+\delta}$ [8] exhibit visible-light photocatalytic activity and superconductivity, respectively.

Figure 1. Structure of the ideal perovskite structure, $A_{n-1}B_nO_{3n+1}$ (*n* = 1, 2, ∞).

ABO_3 (*n* = ∞) A_2BO_3 (*n* = 1) $A_3B_2O_7$ (*n* = 2)
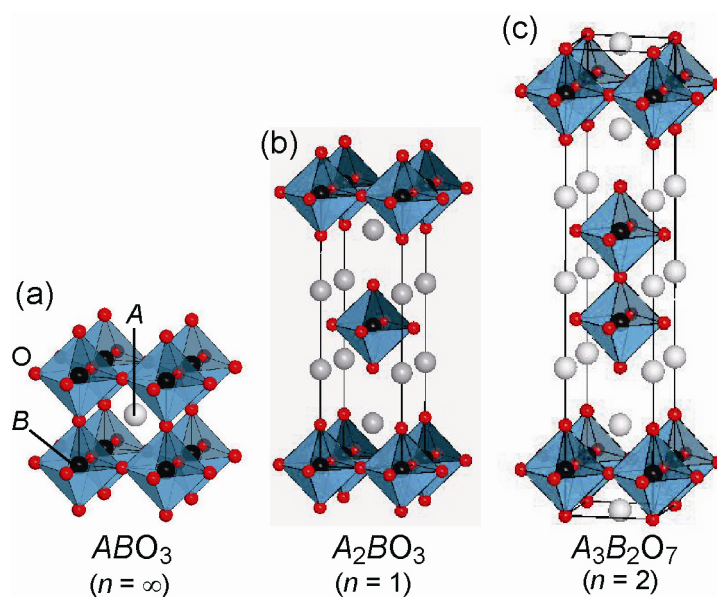
In general, it is very difficult to stabilize two kinds of hetero anions in one structure using conventional solid-state reactions, in comparison with compounds with a single anion, such as an oxide, sulfide or nitride. As for the oxyfluoride compounds, several synthetic approaches are employed to overcome the problem, namely a low-temperature reaction using fluorinating agents [8–11],

hydrothermal reaction [12] or high-pressure synthesis [13,14]. Interestingly, O/F site order and/or F contents inserted, which are closely correlated with the structural and physical properties, depend on the reaction method used. In particular, layered perovskite structures exhibit three types of anion distribution patterns; (i) regular or random anion occupation pattern in the perovskite blocks, (ii) fluorine insertion into only interstitial sites between the perovskite blocks, or (iii) fluorine occupation of both the terminal apical sites and the interstitial sites. In this paper, we first review recent progress in the oxyfluoride chemistry of perovskite-based compounds, then present a synthesis strategy to further extend layered perovskite systems.

2. Fluorine Occupation Patterns in Layered Oxyfluoride Perovskite

2.1. Regular or Random Anion Occupation Pattern in the Perovskite Blocks

Early in the study on the layered oxyfluoride perovskite, high temperature solid-state reaction, one of the easiest synthetic methods, was commonly employed. However, the variety of transition metals in the reported oxyfluoride compounds is quite limited, mainly due to the high chemical stability of the simple starting fluoride materials. To the best of our knowledge, the first example of the RP-type layered perovskite compound is K_2NbO_3F, which was reported in 1962 by Galasso and Darby [15]. As shown in Figure 2(a), the niobium oxyfluoride adopts the tetragonal structure in the space group of *I*4/*mmm* with octahedral coordination around Nb atom and O/F site disorder at the apical sites. The preferential occupation of the fluoride anion at the apical sites elongated the Nb-O/F bonds (2.0642 Å) along the *c* axis compared with those (1.9780 Å) in the *ab* plane. Subsequently, the same authors reported an isostructural iron oxyfluoride, Sr_2FeO_3F [16] and determined the crystal structure to be *I*4/*mmm*. However, Weller and his collaborators demonstrated that the exact crystal symmetry could be described as *P*4/*nmm* [17]. In contrast to K_2NbO_3F, the Fe counterpart possesses the O/F site order at the apical sites leading to a strong distortion of the FeO_5F octahedron (see Figure 2(b)). In fact, the bond length between Fe and O or F is 1.904 or 2.730 Å. Therefore, the iron metal center effectively takes a square pyramidal coordination against five O^{2-} anions. Weller *et al.* also extended the layered oxyfluoride system to Ba_2BO_3F (*B* = Sc and In) [18]. Both compounds exhibit preferential occupation by F^- anions at the apical sites, but the anion-site order/disorder in *B* = In/Sc.

In addition to the RP-type layered perovskite, Dion-Jacobson (DJ) and Aurivillius (AV) -type layered oxyfluoride phases are reported. The formulas of DJ and AV phases are expressed as $AA'_{n-1}B_nO_{3n+1}$ and $(Bi_2O_2)(A'_{n-1}B_nO_{3n+1})$, respectively. $A SrNb_2O_6F$ (*A* = Li, Na, Rb) [19] (Figure 3) and $RbLnTiNbO_6F$ (*Ln* = La, Pr, Nd) [20] were synthesized by conventional solid-state reaction. In contrast to the above RP phases, the F atoms prefer to occupy the equatorial and central apical anion sites in the double-layered perovskite block, not the terminal apical ones, because the covalency of the chemical bond between Nb and the terminal apical oxygen is incompatible with the ionicity of the Nb-F bond. On the other hand, Kobayashi *et al.* reported the reductive fluorination of DJ-$RbLaNb_2O_7$ and RP-$NaYTiO_4$ into $RbLaNb_2O_{7-x}F_x$ and $NaYTiO_{4-x}F_x$ using poly(vinylidene)fluoride (PVDF) [21]. PVDF or poly(tetrafluoroethylene) (PTFE) are effective fluorinating agents, utilized by Slater for the first time [11]. This fluorination proceeds in a topotactic manner; the framework of the precursor is maintained through the reaction. While $A SrNb_2O_6F$ and $RbLnTiNbO_6F$ with the non-magnetic *B*

cations are insulating, RbLaNb$_2$O$_{7-x}$F$_x$ possesses mixed valence states between Nb^{4+} and Nb^{5+} cations, which makes it electrically conductive.

Figure 2. Crystal structure of (**a**) K$_2$NbO$_3$F, (**b**) Sr$_2$FeO$_3$F, and (**c**) Sr$_2$CoO$_3$F. Solid line represents the unit cell.
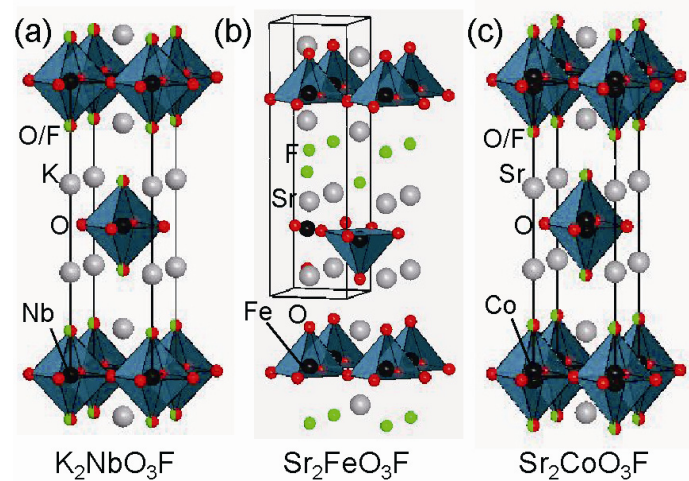
Figure 3. Crystal structure of (**a**) RbSrNb$_2$O$_6$F and (**b**) LiSrNb$_2$O$_6$F.
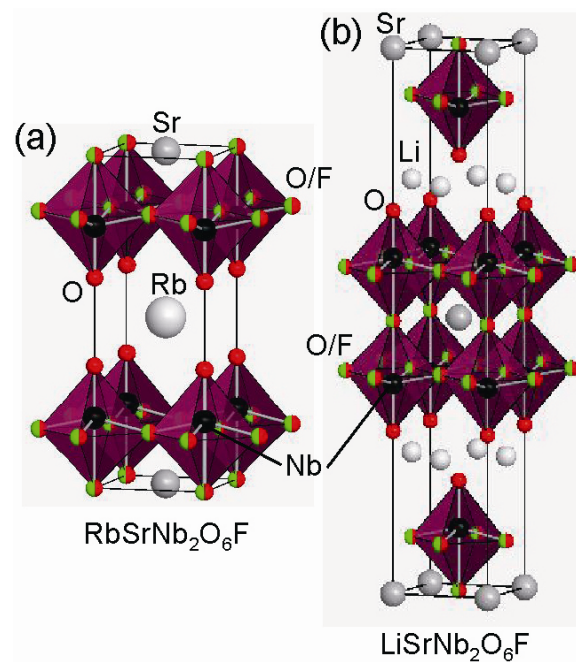
For *n* = 2 RP-type layered perovskite, Ba$_3$In$_2$O$_5$F$_2$ [22] and Sr$_3$Fe$_2$O$_6$F$_{0.68}$ [17] are known. Common to both compounds, fluorine atoms occupy the terminal apical sites. In comparison with Ba$_3$In$_2$O$_5$F$_2$, synthesized by conventional high-temperature reaction, Sr$_3$Fe$_2$O$_6$F$_{0.68}$ is obtained by a low-temperature fluorination using F$_2$ gas. As shown in Figure 4, the precursor Sr$_3$Fe$_2$O$_6$ has an oxygen vacancy at the central apical site, but its oxidative fluorination causes local migration of the terminal apical site to the original oxygen vacant site. Because the intercalated F atoms occupy the terminal apical sites with O, the deviation of the O-Fe-O bond angle in the plane from the ideal 180° is only 7.6°, much smaller

than the corresponding value of 15.28° in $Ba_3In_2O_5F_2$ with full fluorine occupation of the terminal apical sites.

Figure 4. Crystal structure of (**a**) $Sr_3Fe_2O_6$ and (**b**) $Sr_3Fe_2O_6F_{0.86}$. (**c**) Fluorination process of $Sr_3Fe_2O_6$ to $Sr_3Fe_2O_6F_{0.86}$, showing rearrangement of oxide and fluoride anions.
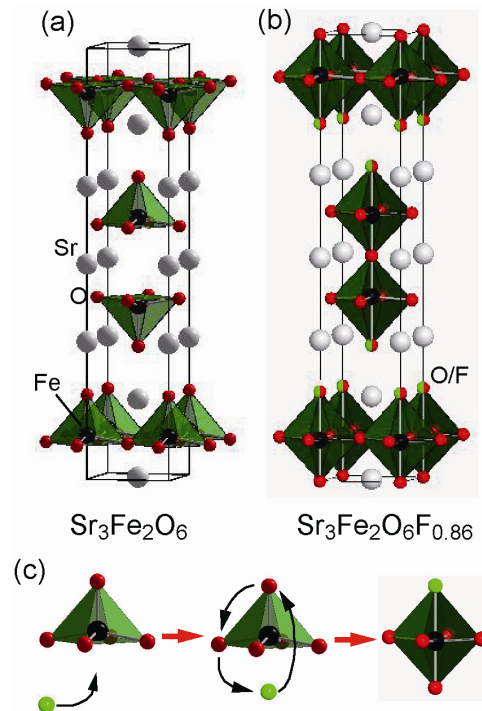
Figure 5. Crystal structure of (**a**) $Bi_2TiO_4F_2$, and (**b**) Bi_2NbO_5F.
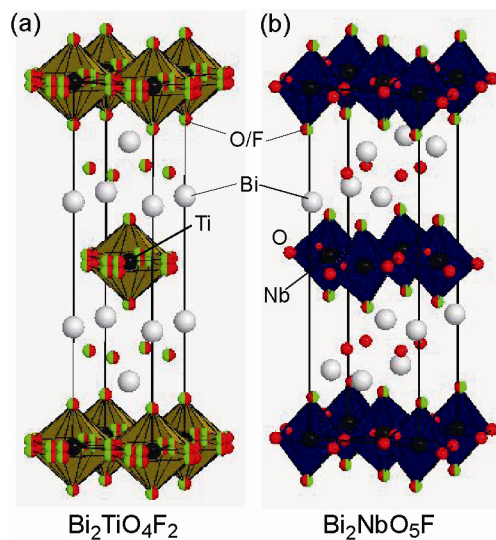
Three kinds of AV-type layered oxyfluoride perovskites, Bi_2BO_5F (B = Nb, Ta) and $Bi_2TiO_4F_2$ (Figure 5), were synthesized by Aurivillius [23]. Later work presented the ferroelectric phase transitions at T_C = 303, 283, and 284 K, respectively, but the relationship between the crystal structure and the ferroelectricity is still controversial. Hydrothermal synthesis yields better sample quality than conventional solid-state reaction [24]. $Bi_2TiO_4F_2$ adopts the simple body-centered tetragonal structure in the space group *I4/mmm* [24] while Bi_2NbO_5F is proposed to adopt *Pbca* symmetry [25]. These

centrosymmetric crystal structures contradict the requirement for the ferroelectricity. In fact, the reexamination of electrical properties in Bi_2NbO_5F demonstrated neither second-harmonic generation nor a permittivity anomaly associated with ferroelectric phase transition reported previously. It is believed from bond-valence-sum calculations that F atoms tend to occupy the equatorial sites for $Bi_2TiO_4F_2$ or the apical sites for Bi_2NbO_5F.

We would like to show a new class of anion ordered perovskite materials, $KNaNbOF_5$ and $KNaMO_2F_4$ ($M = Mo^{6+}$, W^{6+}) expressed as the general formula $ABB'(O,F)_6$ [12]. Poeppelmeier *et al.* successfully synthesized these three compounds by hydrothermal reaction. Layers of K^+ cations and cation vacancies are alternately located in the *A* site along the *c* axis, and Na^+ and *B* (Nb^{5+}, Mo^{6+}, W^{6+}) cations are ordered in a rock salt configuration. More interestingly, fluoride anions are located in K^+ cation layers while apical oxide anions are located in the adjacent *A*-site layer containing the *A*-site vacancies. Similar to DJ-$ASrNb_2O_6F$, the Nb^{5+} cation form short Nb=O bonds and one long Nb-F bond opposite the O^{2-} anion, leading to strong distortion of the Nb^{5+}-centered octahedron. This type of O/F anion order has never been seen in any other oxyfluorides. It is apparent that the cation order in both *A* and *B* sites influences the O/F anion order.

2.2. Fluorine Insertion into Only Interstitial Sites between the Perovskite Blocks

There are a few examples that involve fluorine insertion into only interstitial sites between the perovskite block layers. The RP-type layered manganese oxides, $LaSrMnO_4$ ($n = 1$) and $Ln_{1.2}Sr_{1.8}Mn_2O_7$ (Ln = Pr, Nd, Sm, Eu, and Gd) ($n = 2$), accommodate fluorine in the (La/Sr)O rock-salt layers between the Mn-O perovskite blocks, followed by large expansion of the *c*-axis of $1 \sim 3$ Å (see Figure 6). Utilization of F_2 gas, NH_4F, CuF_2 or PVDF as a fluorination agent at low temperatures yields $LaSrMnO_4F_2$ [26,27] and $Ln_{1.2}Sr_{1.8}Mn_2O_7F_2$ [26,28] where fluorine is inserted in each perovskite block. In addition, heating these fluorinated compounds with the corresponding precursors in appropriate ratios results in a staged intercalation structure, namely $LaSrMnO_4F$ [27,29] and $La_{1.2}Sr_{1.8}Mn_2O_7F$ [27] where F is inserted between alternate rock-salt layers. It should be noted that the F sites in the rock-salt layers are different between $LaSrMnO_4F$ and $LaSrMnO_4F_2$, and $La_{1.2}Sr_{1.8}Mn_2O_7F$ and $Ln_{1.2}Sr_{1.8}Mn_2O_7F_2$; the F atoms in $LaSrMnO_4F$ and $La_{1.2}Sr_{1.8}Mn_2O_7F$ are located in the interlayer space so as to bridge between La/Sr and the apical oxygen, while the F atoms in $LaSrMnO_4F_2$ and $Ln_{1.2}Sr_{1.8}Mn_2O_7F_2$ occupy tetrahedral sites of $(La/Sr)_4$ in the rock-salt layers. In spite of the valences of Mn cations close to 4+, no long-range magnetic order is observed down to 5 K.

The $n = 2$ RP phase $Sr_3Ru_2O_7$ is also fluorinated using CuF_2 to give the oxyfluoride $Sr_3Ru_2O_7F_2$ [30]. In the fluorinated phase, fluorine is inserted in the tetrahedral sites of Sr_4 in rock-salt layers between perovskite blocks (see Figure 7). The precursor crystallizes in the tetragonal structure with $I4/mmm$, but the fluorine insertion lowers the crystal symmetry to orthorhombic symmetry (*Pbam*), which is associated with rotation and tilting of the RuO_6 octahedra. The magnetic properties also change after the fluorination reaction, from the ferromagnetic state with T_C = 105 K to weak ferromagnetic state with T_N = 185 K.

Figure 6. Crystal structure of (**a**) $La_{1.2}Sr_{1.8}Mn_2O_3F$, and (**b**) $La_{1.2}Sr_{1.8}Mn_2O_3F_2$.
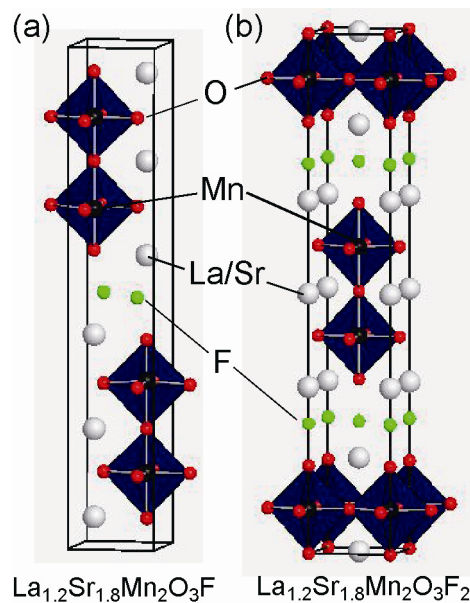
Figure 7. Crystal structure of $Sr_3Ru_2O_7F_2$.
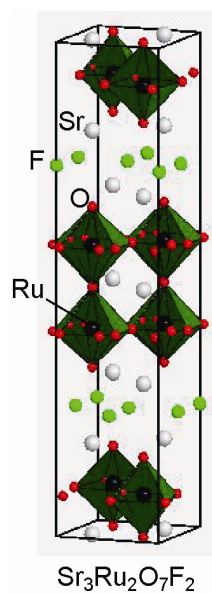
Fluorination of the RP-$Ba_{2-x}Sr_xPdO_3$ ($0 \leq x \leq 1.5$) by PVDF involves unusual oxygen displacement through anion exchange [31,32], which is different from the case of the fluorination of $Sr_3Fe_2O_6$ described above [17]. As shown in Figure 8, the structure of $Ba_{2-x}Sr_xPdO_3$ comprises corner-linked chains of PdO_4 squares along the *a*-axis, similar to the one-dimensional structure in Sr_2CuO_3. Fluorination to $Ba_{2-x}Sr_xPdO_2F_2$ involves structural conversion to *T'*-structure (isostructural with Nd_2CuO_4), namely rearrangement of the PdO_4 network from a 1-D chain to a 2-D plane. The remaining O^{2-} anions in the apical site move to the original vacant site and the two inserted F^- anions build fluorite block layer with Ba/Sr cations. Because the Pd^{2+} cation exhibits a strong preference for square lattice geometry, no additional fluorine insertion at the apical sites is allowed.

Figure 8. (**a**), (**b**), (**c**) Fluorination of A_2BO_3 to $A_2BO_2F_{2-\delta}$ (A = Sr, Ba; B = Cu, Pd). (**d**) Rearrangement of oxide and fluoride anions during fluorination reaction.
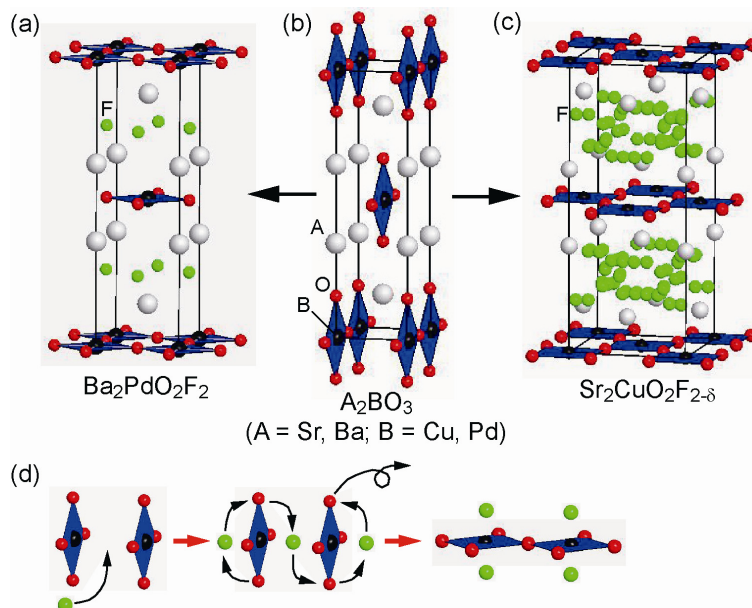
2.3. Fluorine Occupation of Both the Terminal Apical Sites and the Interstitial Sites

In most cases, low-temperature fluorination in layered perovskite structure proceeds by anion substitution at the apical sites and fluorine insertion in interstitial sites between perovskite blocks. This type of fluorination, especially in Cu oxides, has already been reviewed in detail by Greaves *et al.* and Wiley *et al.*, independently [33–35], so we will present the following four examples in this paper, namely $Sr_2CuO_2F_{2+\delta}$ [8,36], $Ba_2ZrO_3F_2 \cdot xH_2O$ [37], $Sr_2TiO_3F_2$ [38], and nitride-fluoride $Ce_2MnN_3F_{2-\delta}$ [39].

The discovery of a superconducting copper oxyfluoride $Sr_2CuO_2F_{2+\delta}$ by Greaves *et al.* triggered the search for new oxyfluoride perovskite materials by a low-temperature route [8]. Other fluorinating agents, such as NH_4F and XeF_2, were shown to be useful in later work [9,10]. This compound was initially obtained by reaction of a 1-D structure Sr_2CuO_3 with F_2 gas. As observed in $Ba_{2-x}Sr_xPdO_2F_2$ [31], the network of corner-sharing CuO_4 units drastically changes from a 1-D chain to a 2-D layer in the fluorination process (see Figure 8). However, fluorine anions partially occupy not only interstitial sites between the perovskite blocks but also the apical sites. The superconducting temperature takes a maximum value of $T_C = 46$ K at $\delta \sim 0.3$. Interestingly, reduction of $Sr_2CuO_2F_{2+\delta}$ in a flowing H_2/N_2 gas atmosphere yields an insulating T'-structure $Sr_2CuO_2F_2$ [36]; fluorine removal at the apical sites and rearrangement of the remaining F^- anions form a fluorite Sr_2F_2 layer and square planar coordinated CuO_4.

$Sr_2TiO_3F_2$ or $Ba_2ZrO_3F_2 \cdot xH_2O$ can be prepared by the reaction of $n = 1$RP Sr_2TiO_4 or Ba_2ZrO_4 with NH_4F, CuF_2, ZnF_2 or PVDF [37,38]. In both cases, fluorination occurs by substitution of two F^- anions for one O^{2-} anion, but the fluorine insertion manner and coordination environment around the metal center are different between these two compounds (see Figure 9). Fluoride anions in $Sr_2TiO_3F_2$ occupy both the apical sites and interstitial sites in alternate rock-salt layers. Additionally, the TiO_5F octahedron is highly distorted, probably due to O/F site order at the apical sites. In contrast, $Ba_2ZrO_3F_2 \cdot xH_2O$

possesses fluorine, located at the apical sites and in each rock-salt layer. The Zr metal center takes an octahedral coordination, with O/F anions being disordered at the apical sites.

Figure 9. Crystal structure of (**a**) $Sr_2TiO_3F_2$, (**b**) $Ba_2ZrO_3F_2 \cdot xH_2O$, and (**c**) $Ce_2MnN_3F_{2-\delta}$.
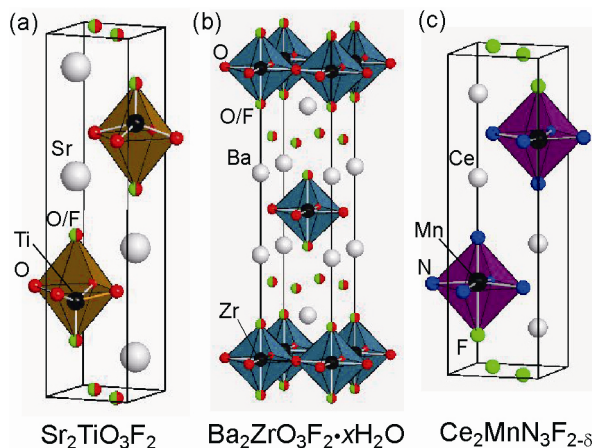
It is important to note that a RP-type layered manganese nitride Ce_2MnN_3, which is isostructural with Sr_2CuO_3, accommodates fluorine in a different way [39]. Unlike $Sr_2CuO_2F_{2+\delta}$ and $Ba_{2-x}Sr_xPdO_2F_2$, fluorination involves local migration of the original apical oxygen to the equatorial anion vacant sites, but anion substitution or oxygen removal does not take place. Moreover, additional fluorine atoms are incorporated in alternate rock-salt layers. The resultant structure resembles that of $Sr_2TiO_3F_2$ and the N/F site order results in deformation of the MnN_4F octahedron. Upon fluorination, the magnetic properties changes the Pauli paramagnetic behavior to a paramagnetic one.

3. Recent Results on New Layered Iron and Cobalt Oxyfluoride Compounds

3.1. Unusual O/F Site Disorder in Layered Cobalt Oxyfluoride

As reviewed above, a variety of fluorinating agents greatly contributes to oxyfluoride chemistry. Considering the limited variety of transition metals, however, a further search for new oxyfluoride phase is necessary in order to better understand oxyfluoride. Co is among the 3d transition metals studied to a lesser extent. In fact, only one Co-based perovskite compound has been reported: $LaSrCoFeO_5F$ [40], where O/F sites are randomly distributed as well as Fe/Co sites. High-pressure synthesis is an effective alternative approach to low-temperature fluorination, although expensive apparatus required for the reaction method is necessary. Recently, we have achieved the synthesis of the first example of RP-type layered cobalt oxyfluoride Sr_2CoO_3F, under a pressure of 6 GPa at 1,700 °C [41]. This compound adopts a simple body-centered tetragonal structure with the space group *I*4/*mmm* (Figure 2(c)). Magnetic susceptibility measurements revealed an antiferromagnetic phase transition at around 320 K, which is different from the ferromagnetic behavior in the corresponding oxide Sr_2CoO_4 [42]. Furthermore, neutron powder diffraction study characterized the $S = 2$ high-spin state at Co cations. The structural features in the cobalt oxyfluoride are also worthy of attention. The O/F anions are disordered at the apical sites, and the cobalt cation shifted from the basal plane takes a square pyramidal coordination. We noticed that the coordination environment around Co center is

unusual when compared with related oxyfluoride compounds (see Figure 2). As described above, a similar O/F site disorder is observed in Ba_2ScO_3F and K_2NbO_3F, but each *B* cation with d^0 electronic configuration takes octahedral coordination without shifting from the basal plane. In comparison, Sr_2FeO_3F and Ba_2InO_3F have a square-pyramidal coordinated metal center, but O/F site occupation occurs in an ordered manner. Thus, coexistence of anion disorder and square-pyramidal coordination, which has never seen in related oxyfluoride, is realized in the new cobalt oxyfluoride. It was initially assumed that square-pyramidal coordination stabilizes the O/F site ordered state, but this is not the case in Sr_2CoO_3F. Square-pyramidal coordination of Co cations is commonly seen in cobalt-based materials with d^6 high spin configuration, such as $BiCoO_3$ [43] and Sr_2CoO_3Cl [44]. The observed O/F disorder, however, is non-trivial. The role played in the unusual coordination environment around Co is probably related to the reaction condition employed: high-pressure and high-temperature synthesis. A denser environment at high pressure or entropic effects associated with high temperature are likely to stabilize the anion-disordered phase.

3.2. Highly Fluorinated Iron Oxides

Various fluorinating agents have been reported so far, for example, F_2 gas, NH_4F, XeF_2, CuF_2 and PVDF and PTFE [8–11,21]. Each fluorinating agent exhibits a distinct fluorinating power and reaction pathway. Thus, the fluorine contents in the resultant material depend on the choice, not only of the fluorinating agent, but also the anion lattice of the precursors. For example, the fluorine contents incorporated by XeF_2 in $YBa_2Cu_3O_{7-\delta}$ increase with decreasing the oxygen deficient contents [45]. The fluorination of perovskite $SrFeO_3$ using PVDF yields $SrFeO_2F$ while the reaction of brownmillerite $Sr_2Fe_2O_5$ with F_2 gas results in the formation of two cubic phases different from $SrFeO_2F$ [17,46].

On the other hand, as shown above, the $n = 2$ RP-type layered iron oxide $Sr_3Fe_2O_6$ was fluorinated with F_2 gas to give the oxyfluoride $Sr_3Fe_2O_6O_{0.87}$ [17]. This fluorination did not involve anion substitution. There are two approaches to extending the fluorine contents; a precursor with smaller oxygen concentrations is reacted with F_2 gas, or a fluorinating agent with higher reducing power is employed. According to such perspectives, we successfully synthesized a more highly fluorinated iron oxide, $Sr_3Fe_2O_{5.44}F_{1.56}$, by reaction of $Sr_3Fe_2O_{7-\delta}$ ($\delta\sim0.25$) [47]. As is the case in $Sr_3Fe_2O_6O_{0.87}$, fluoride anions preferentially occupy the terminal apical anion sites with oxide anions, but the O/F sites are displaced from the ideal $4e$ $(0, 0, z)$ to more general sites $16m$ (x, x, z). Moreover, fluorination with PTFE results in more significant expansion of the *c*-axis (21.406(2) Å) and the deviation of the O-Fe-O bond angle in the plane from 180° is 15.28° nearly close to that in $Ba_3In_2O_5F_2$, reflecting the increased fluorine content in $Sr_3Fe_2O_{5.44}F_{1.56}$. And, the antiferromagnetic phase transition temperature greatly differs from below r.t. to 390 K.

Interestingly, work that is more recent has demonstrated further extended fluorination. Slater *et al.* have successfully synthesized three more fluorinated phases, $Sr_3Fe_2O_{5.28}F_{1.72}$, $Sr_3Fe_2O_4F_4$, and $Sr_3Fe_2O_3F_6$, by changing the molar ratios of $Sr_3Fe_2O_{7-\delta}$ to PVDF [48]. While $Sr_3Fe_2O_{5.28}F_{1.72}$ has structural features similar to $Sr_3Fe_2O_{5.44}F_{1.56}$, fluorine atoms in $Sr_3Fe_2O_4F_4$ occupy half interstitial sites between rock-salt layers as well as terminal and central anion sites (see Figure 10). These two compounds exhibit antiferromagnetic order at r.t. In contrast, $Sr_3Fe_2O_3F_6$, which is assumed to

correspond to complete filling of both apical sites and interstitial sites by fluorine, magnetically orders below r.t.

Figure 10. Crystal structure of (**a**) $Sr_3Fe_2O_{5.44}F_{1.56}$, and (**b**) $Sr_3Fe_2O_4F_4$.
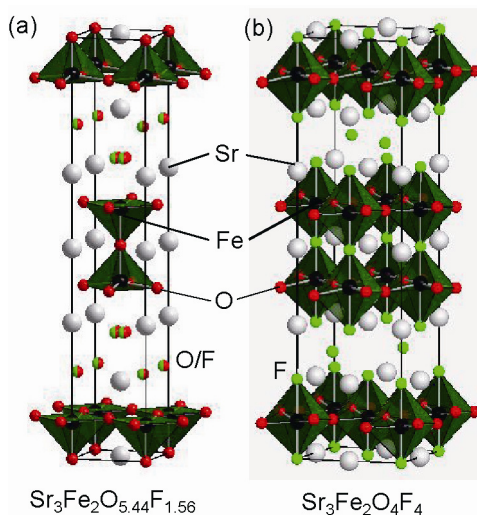
5. Conclusions

We have reviewed how layered oxyfluoride perovskite compounds have a rich variety of fluorine occupation, depending on reaction route, namely, low-temperature reaction, hydrothermal reaction, and high-pressure synthesis. Low temperature topotactic reaction is an attractive and straightforward technique to synthesize kinetically stable phases; Not only anion substitution but also fluorine insertion in interstitial sites between perovskite blocks occur, in some cases involving a rearrangement of anions around the metal center. In particular, the high capacity for fluorine insertion observed in $Sr_3Fe_2O_{7-\delta}$ is quite unusual compared with other metal oxides. High-pressure synthesis can also provide good opportunities for extending oxyfluoride chemistry. Indeed, an unusual coordination environment in Sr_2CoO_3F was realized under extreme experimental conditions. This result should contribute not only to further syntheses of new oxyfluoride compounds, but also to controlling the structural and physical properties through anion order/disordering.

Acknowledgments

References

1. Bednorz, J.G.; Müller, K.A. Possible high Tc superconductivity in the Ba-La-Cu-O. *Z. Phys. B* **1986**, *64*, 189–193.
2. Urushibara, A.; Moritomo, Y.; Arima, T.; Asamitsu, A.; kido, G.; Tokura, Y. Insulator-metal transition and giant magnetoresistance in $La_{1-x}Sr_xMnO_3$. *Phys. Rev. B* **1995**, *51*, 14103–14109.
3. Moritomo, Y.; Asamitsu, A.; Kuwahara, H.; Tokura, Y. Giant magnetoresistance of manganese oxides with a layered perovskite structure. *Nature* **1996**, *380*, 141–144.
4. Tokura, Y.; Nagaosa, N. Orbital physics in transition-metal oxides. *Science* **2000**, *288*, 462–468.
5. Cava, R.J. Oxide superconductors. *J. Am. Ceram. Soc.* **2000**, *83*, 1–28.
6. Dagotto, E. Correlated electrons in high-temperature superconductors. *Rev. Mod. Phys.* **1994**, *66*, 763–841.
7. Kasahara, A.; Nukumizu, K.; Hitoki, G.; Takata, T.; Kondo, J.N.; Hara, M.; Kobayashi, H.; Domen, K. Photoreaction on $LaTiO_2N$ under visible light irradiation. *J. Phys. Chem. A* **2002**, *106*, 6750–6753.
8. Al-Mamouri, M.; Edwards, P.P.; Greaves, C.; Slaski, M. Synthesis and superconducting properties of the strontium copper oxy-fluoride $Sr_2CuO_2F_{2+\delta}$. *Nature* **1994**, *369*, 382–384.
9. Slater, P.R.; Hodges, J.P.; Francesconi, M.G.; Edwards, P.P.; Greaves, C.; Gameson, I.; Slaski, M. An improved route to the synthesis of superconducting copper oxyfluorides $Sr_{2-x}A_xCuO_2F_{2+\delta}$ (A = Ca, Ba) using transition metal difluorides as fluorinating reagents. *Phys. C* **1995**, *253*, 16–22.
10. Ardashnikova, E.I.; Lubarsky, S.V.; Denisenko, D.I.; Shpanchenko, R.V.; Antipov, E.V.; van Tendeloo, G. A new way of synthesis and characterization of superconducting oxyfluoride $Sr_2Cu(O, F)_{4+\delta}$. *Phys. C* **1995**, *253*, 259–265.
11. Slater, P.R. Poly(vinylidene fluoride) as a reagent for the synthesis of K_2NiF_4-related inorganic oxide fluorides. *J. Fluor. Chem.* **2002**, *117*, 43–45.
12. Pinlac, R.A.; Stern, C.L.; Poeppelmeier, K.R. New layered oxide-fluoride perovskites: $KNaNbOF_5$ and $KNaMO_2F_4$ ($M = Mo^{6+}$, W^{6+}). *Crystals* **2011**, *1*, 3–14.
13. Troyanchuk, I.O.; Kasper, N.V.; Mantytskaya, O.S.; Shapovalova, E.F. High-pressure synthesis of some perovskite-like compounds with a mixed anion type. *Mater. Res. Bull.* **1995**, *30*, 421–425.
14. Katsumata, T.; Nakashima, M.; Umemoto, H.; Inaguma, Y. Synthesis of the novel perovskite-type oxyfluoride $PbScO_2F$ under high pressure and high temperature. *J. Solid State Chem.* **2008**, *181*, 2737–2740.
15. Galasso, F.; Darby, W. Preparation, structure, and properties of K_2NbO_3F. *J. Phys. Chem.* **1962**, *66*, 1318–1320.
16. Galasso, F.; Darby, W. Preparation and properties of Sr_2FeO_3F. *J. Phys. Chem.* **1963**, *67*, 1451–1453.
17. Case, G.S.; Hector, A.L.; Levason, W.; Needs, R.L.; Thomas, M.F.; Weller, M.T. Synthesis powder neutron diffraction structures and Mössbauer studies of some complex iron oxyfluorides: $Sr_3Fe_2O_6F_{0.87}$, Sr_2FeO_3F and $Ba_2InFeO_5F_{0.68}$. *J. Mater. Chem.* **1999**, *9*, 2821–2827.
18. Needs, R.L.; Weller, M.T.; Scheler, U.; Harris, R.K. Synthesis and structure of Ba_2InO_3X (X = F, Cl, Br) and Ba_2ScO_3F; oxide/halide ordering in K_2NiF_4-type structures. *J. Mater. Chem.* **1996**, *6*, 1219–1224.

19. Choy, J.H.; Kim, J.Y.; Kim, S.J.; Sohn, J.S. New Dion-Jacobson-type layered perovskite oxyfluorides, $ASrNb_2O_6F$ (A = Li, Na, and Rb). *Chem. Mater.* **2001**, *13*, 906–912.

20. Caruntu, G.; Spinu, L.; Wiley, J.B. New rare-earth double-layered-perovskite oxyfluorides, $RbLnTiNbO_6F$ (Ln = La, Pr, Nd). *Mater. Res. Bull.* **2002**, *37*, 133–140.

21. Kobayashi, Y.; Tian, M.; Eguchi, M.; Mallouk, T. Ion-exchangeable, electronically conducting layered perovskite oxyfluorides. *J. Am. Chem. Soc.* **2009**, *131*, 9849–9855.

22. Needs, R.L.; Weller, M.T. Structure of $Ba_3In_2O_5F_2$ by combined powder analysis; oxide/fluoride ordering in a Ruddlesden-Popper phase. *J. Chem. Soc. Dalton Trans.* **1995**, *18*, 3015–3017.

23. Aurivillius, B. The structure of Bi_2NbO_5F and isomorphous compounds. *Ark. Kemi.* **1952**, *5*, 39–47.

24. Needs, R.L.; Dann, S.E.; Weller, M.T. Cherryman, J.C.; Harris, R.K. The structure and oxide/fluoride ordering of the ferroelectrics $Bi_2TiO_4F_2$ and Bi_2NbO_5F. *J. Mater. Chem.* **2005**, *15*, 2399–2407.

25. McCabe, E.E.; Jones, I.P.; Zhang, D.; Hyatt, N.C.; Greaves, C. Crystal structure and electrical characterization of Bi_2NbO_5F: An Aurivillius oxide fluoride. *J. Mater. Chem.* **2007**, *17*, 1193–1200.

26. Greaves, C.; Kissick, J. L.; Francesconi, M.G.; Aikens, L.D. Gillie, L.J. Synthetic strategies for new inorganic oxide fluorides and oxide sulfates. *J. Mater. Chem.* **1999**, *9*, 111–116.

27. Aikens, L.D.; Gillie, L.J.; Li, R.K.; Greaves, C. Staged fluorine insertion into manganese oxides with Ruddlesden-Popper structures: $LaSrMnO_4F$ and $La_{1.2}Sr_{1.8}MnO_2O_7F$. *J. Mater. Chem.* **2002**, *12*, 264–267.

28. Sivakumar, T.; Wiley, J.B. Topotactic route for new layered perovskite oxides containing fluorine: $Ln_{1.2}Sr_{1.8}Mn_2O_7F_2$ (Ln = Pr, Nd, Sm, Eu, and Gd). *Mater. Res. Bull.* **2009**, *44*, 74–77.

29. Aikens, L.D.; Li, R.K.; Greaves, C. The synthesis and structure of a new oxide fluoride, $LaSrMnO_4F$, with stated fluorine insertion. *Chem. Commun.* **2000**, 2149–2130.

30. Li, R.K.; Greaves, V. Double-layered ruthenate $Sr_3Ru_2O_7F_2$ formed by fluorine insertion into $Sr_3Ru_2O_7$. *Phys. Rev. B* **2000**, *62*, 3811–13815.

31. Baikie, T.; Dixon, E.L.; Rooms, J.F.; Young, N.A.; Francesconi, M.G. $Ba_{2-x}Sr_xPdO_2F_2$ ($0 \leq x \leq 1.5$): The first palladium-oxide-fluoride. *Chem. Commun.* **2003**, 1580–1581.

32. Baikie, T.; Islam, M.S.; Francesconi, M.G. Defects in the new oxide-fluoride $Ba_2PdO_2F_2$: The search for fluoride needles in an oxide haystack. *J. Mater. Chem.* **2005**, *15*, 119–123.

33. Greaves, C.; Fracesconi, M.G. Fluorine insertion in inorganic materials. *Curr. Opni. Solid State Mater. Sci.* **1998**, *3*, 132–136.

34. McCabe, E.E. Greaves, C. Fluorine insertion reactions into preformed metal oxides. *J. Fluor. Chem.* **2007**, *128*, 448–458.

35. Sanjaya Ranmohotti, K.G.; Josepha, E.; Choi, J.; Zhang, J.; Wiley, J.B. Topochemical manipulation of perovskites: Low-temperature reaction strategies for directing structure and properties. *Adv. Mater.* **2011**, *23*, 442–460.

36. Kissick, J.L.; Greaves, C.; Edwards, P.P.; Cherkashenko, V.M.; Kurmaev, E.Z.; Bartkowski, S.; Neumann, M. Synthesis, structure, and XPS characterization of the stoichiometric phase $Sr_2CuO_2F_2$. *Phys. Rev. B* **1997**, *56*, 2831–2835.

37. Slater, P.R.; Gover, R.K.B. Synthesis and structure of the new oxide fluoride $Ba_2ZrO_3F_2 \cdot xH_2O$. *J. Mater. Chem.* **2001**, *11*, 2035–2038.

38. Slater, P.R.; Gover, R.K.B. Synthesis and structure of the new oxide fluoride $Sr_2TiO_3F_2$ from the low temperature fluorination of Sr_2TiO_4: An example of a staged fluorine substitution/insertion reaction. *J. Mater. Chem.* **2002**, *12*. 291–294.

39. Headspith, D.A.; Sullivan, E.; Greaves, C.; Francesconi, M.G. Synthesis and characterization of the quaternary nitride-fluoride $Ce_2MnN_3F_{2-\delta}$. *Dalton Trans.* **2009**, 9273–9279.

40. El Shinawi, H; Marco, J.F.; Berry, F.J.; Greaves, C. $LaSrCoFeO_5$, $LaSrCoFeO_5F$ and $LaSrCoFeO_{5.5}$: New La-Sr-Co-Fe perovskites. *J. Mater. Chem.* **2010**, *20*, 3253–3259.

41. Tsujimoto, Y.; Li, J.J.; Yamaura, K.; Matsushita, Y.; Katsuya, Y.; Tanaka, M.; Shirako, Y.; Akaogi, M.; Takayama-Muromachi, E. New layered cobalt oxyfluoride, Sr_2CoO_3F. *Chem. Commun.* **2011**, *47*. 3263–3265.

42. Wang, X.L.; Takayama-Muromachi, E. Magnetic and transport properties of the layered perovskite system $Sr_{2-y}Y_yCoO_4$ ($0 \leq y \leq 1$). *Phys. Rev. B* **2005**, *72*, doi: 10.1103/PhysRevB.72.064401.

43. Belik, A.A.; Iikubo, S.; Kodama, K.; Igawa, N.; Shamoto, S.; Niitaka, S.; Azuma, M.; Shimakawa, Y.; Takano, M.; Izumi, F.; *et al.* Neutron powder diffraction study on the crystal and magnetic structures of $BiCoO_3$. *Chem. Mater.* **2006**, *18*, 798–803.

44. Loureiro, S.M.; Felser, C.; Huang, Q.; Cava, R.J. Refinement of the crystal structures of strontium cobalt oxychlorides by neutron powder diffraction. *Chem. Mater.* **2000**, *12*, 3181.

45. Shpanchenko, R.V.; Rozova, M.G.; Abakumov, A.M.; Ardashnikova, E.I.; Kovba, M.L.; Putilin, S.N.; Antipov, E.V.; Lebedev, O.I.; Tendeloo, G.V. Inducing superconductivity and structural transformations by fluorination of reduced YBCO. *Phys. C* **1997**, *280*, 272–280.

46. Berry, F.J.; Ren, X.; Hea, R.; Slater, P.; Thomas, M.F. Fluorination of perovskite-related $SrFeO_{3-\delta}$. *Solid State Commun.* **2005**, *134*, 621–624.

47. Tsujimoto, Y.; Yamaura, K.; Hayashi, N.; Kodama, K.; Igawa, N.; Matsushita, Y.; Katsuya, Y.; Shirako, Y.; Akaogi, M.; Takayama-Muromachi, E. Topotactic synthesis and crystal structure of a highly fluorinated Ruddlesden–Popper-type Iron oxide, $Sr_3Fe_2O_{5+x}F_{2-x}$ ($x \approx 0.44$). *Chem. Mater.* **2011**, *23*, 3652–3658.

48. Hancock, C.A.; Herranz, T.; Marco, J.F.; Berry, F.J.; Slater, P.R. Low temperature fluorination of $Sr_3Fe_2O_{7-\delta}$ with polyvinylidine fluoride: An X-ray powder diffraction and Mössbauer spectroscopy study. *J. Solid State Chem.* **2012**, *186*, 195–203.